Materials Letters 203 (2017) 73–76

Contents lists available at ScienceDirect

Materials Letters

journal homepage: www.elsevier.com/locate/mlblue

Sputtered seed-assisted growth of CuS nanosheet arrays as effective counter electrodes for quantum dot-sensitized solar cells

Xiaodan Hong [a], Zijie Xu [a], Fayin Zhang [a,b], Chunfeng He [a], Xiaoyue Gao [a], Qun Liu [a], Wenxi Guo [a], Xiangyang Liu [a,c], Meidan Ye [a,*]

[a] Research Institute for Biomimetics and Soft Matter, Fujian Provincial Key Lab for Soft Functional Materials Research, Department of Physics, College of Physical Science and Technology, Xiamen University, Xiamen 361005, PR China
[b] The State Key Laboratory for Modification of Chemical Fibers and Polymer Materials, College of Materials Science and Engineering, Donghua University, Shanghai 201620, PR China
[c] Department of Physics, Faculty of Science, National University of Singapore, Singapore 117542, Singapore

ARTICLE INFO

Article history:
Received 12 April 2017
Accepted 18 May 2017
Available online 19 May 2017

Keywords:
Copper sulfide
RF sputtering
Quantum dot-sensitized solar cells

ABSTRACT

CuS nanosheet arrays (NSAs) obtained by combining a physical radio frequency (RF) sputtered CuS seeding process with a facile and green hydrothermal post-treatment, are employed as counter electrodes (CEs) for quantum dot-sensitized solar cells (QDSSCs). Such CuS NSAs show superior electrocatalytic ability as compared to the conventional Pt CEs and other three types of CuS nanosheet films prepared via different methods.

1. Introduction

As a well-known p-type semiconductor, copper sulfide has aroused considerable interests because of its stoichiometry-dependent band, low cost, and nontoxic properties as well as its potential applications in photocatalysis, superconductors, especially in solar cells [1]. Compared to traditional noble metal-based counter electrodes (CEs), particularly Pt films, copper sulfide CEs display higher electrocatalytic activity for quantum dot-sensitized solar cells (QDSSCs) with enhanced cell efficiencies [2,3]. To date, multiple routes have been developed in the fabrication of CuS nanocrystals, such as sacrificial templating method, wet chemical bath, ultrasonic and microwave irradiation, chemical vapor reaction, electrodeposition and atomic layer deposition [4,5]. However, few articles relating to the facile growth of CuS nanosheet arrays assisting by directly magnetron sputtering CuS target were reported.

As a kind of physical vapor deposition, radio frequency (RF) magnetron sputtering technique has the potential for industrial applications because of its simple devices, low cost, large-scale and strong adhesion between the as-sputtered films and substrates. This kind of physical process is controllable and requires little from the substrates, which make it possible for the deposition on various substrates [6]. Therefore, in this work, the RF magnetron sputtering technique was employed to fabricate the uniform CuS seeds on FTO substrates, followed by a hydrothermal process to grow CuS NSAs on the seeded FTO substrates. Both the CuS seeds and the CuS NSAs were used as CEs in QDSSCs, which then showed higher performance in electrochemically catalyzing S^{2-}, as compared to the conventional Pt films.

2. Experimental section

2.1. Preparation of CuS nanosheet arrays

CuS NSAs were successfully fabricated by the combination of physical (RF sputtering) and chemical (hydrothermal) processes. Firstly, CuS seeds were deposited by applying the radio frequency (RF) magnetron sputtering on clean FTO substrates using the CuS target. And then the CuS seeded FTO substrate was treated by a facile hydrothermal method in aqueous solution with 0.01 M $Cu(NO_3)_2$ and 0.05 M thiourea at 150 °C for 20 h. The FTO substrate was taken out and rinsed with DI water, and dried in air. Finally, the CuS thin films grown on the FTO substrates were obtained. The whole process was displayed in Fig. S1d. For comparison, different methods were also applied to fabricate CuS nanosheets, which were illustrated in Fig. S1a–c.

2.2. Preparation of CdS/CdSe QDSSCs

For QDSSCs (Fig. S2), the photoanode films with a thickness of about 20 μm were obtained by doctor balding P25 paste. And

* Corresponding author.
E-mail address: mdye@xmu.edu.cn (M. Ye).

http://dx.doi.org/10.1016/j.matlet.2017.05.078
0167-577X/

CdS/CdSe co-sensitised QDs were deposited on the photoanode films by chemical bath deposition (CBD) method, similar to our previous work [1].

3. Results and discussions

To study the phase structure of CuS samples, XRD, Raman, and XPS measurements were performed. As shown in Fig. 1a, no typical diffraction peak except for the characteristic peaks of FTO was found, indicating that the 30 min-sputtered CuS seeds (marked as CuS-30 min) were amorphous. Fig. 1b shows the XRD pattern of CuS seeds sputtered on amorphous glass, no typical diffraction emerged once again, further verifying the CuS seeds were amorphous. Fig. 1c displays the XRD patterns of the seed-assisted CuS NSAs (marked as CuS-30 min-hy) which coincided with the standard diffraction peaks of hexagonal CuS (JCPDS No. 06-0464). Other samples obtained by different sputtering time were also tested by XRD measurement, the corresponding results were shown in Fig. S3. All the XRD patterns revealed that the CuS seeds were amorphous while the CuS films were well crystallized.

The Raman spectra (Fig. 1d) of CuS NSAs with a typical peak at around 472 cm^{-1} matched well with the Raman characteristic peak of CuS in literature [7]. In addition, XPS spectrum in the Cu 2p region of CuS NSAs (Fig. 1e) exhibits two main peaks locating at 952.0 eV and 932.2 eV for Cu 2p 1/2 and Cu 2p 3/2, respectively, matching well with the binding energies for Cu 2p. Meanwhile, the peak loaded at 162.0 eV in the S2p XPS spectrum (Fig. 2f) was assigned to S2p binding energy in CuS nanosheets [8].

The morphology of the CuS seeds and CuS NSAs was examined by SEM and TEM measurements. As observed in Fig. 2a–c, the amorphous CuS seeds exhibited no obvious nanostructure. However, the CuS NSAs obtained by the subsequent hydrothermal reaction based on the CuS seeds displayed nanosheet-like shapes and grew perpendicularly on the FTO substrates (Fig. 2d–f). By changing the RF sputtering time, CuS NSAs with different thicknesses and densities were achieved, the thickness of the CuS NSAs increased as the time prolonged. Fig. 2g exhibits the TEM image of a single thin nanosheet, matching well with the SEM image (Fig. 2e). Meanwhile, the lattice spacing of 0.320 nm and 0.301 nm in the HRTEM image could be assigned to the (101) and (102) planes of hexagonal CuS, respectively (Fig. 2h). The selected-area electron diffraction (SAED) pattern (Fig. 2i) shows a bright-dark Laue pattern, suggesting the achievement of single CuS crystals with great crystallinity.

All the samples were fabricated as CEs in QDSSCs. The current density-voltage (J-V) curves of the QDSSCs using Pt and CuS as CEs were shown in Fig. 3a, the corresponding photovoltaic parameters were summarized in Table S1. The short-current density (J_{SC}), open-circuit (V_{OC}), and fill factor (FF) values of the QDSSCs based on a Pt CE as reference were only 11.45 mA/cm^2, 0.47 V and 0.36, respectively, resulting in a quite low PCE value of 1.96%. Compared to the Pt CE, the CuS seed (CuS-30 min) and CuS NSA (CuS-30 min-hy) CEs exhibited relatively higher J_{SC} values of 14.38 mA/cm^2 and 16.37 mA/cm^2, V_{OC} values of 0.48 V and 0.51 V, and FF values of 0.45 and 0.46, consequently contributing to considerable PCE values of 3.08% and 3.83% for the resulting QDSSCs (Fig. 3a and Table S1), respectively.To exam the electrochemical properties of the CuS samples, cyclic voltammetry (CV), EIS and Tafel polarization analysis were performed. The peak in CV curves reflects the redox reaction between electrode materials and polysulfide electrolyte. As shown in Fig. 3b, CuS NSAs displayed a higher current density compared to CuS seeds and Pt electrode at reductive potentials, indicating its best catalytic activity to reduce S_n^{2-} to S^{2-}, matching well with the J-V results. Fig. 3c displays the Nyquist plots fitted by the inset equivalent circuit and the results were listed in Table S1. Compared to R_{CT} value of Pt electrode (1726 Ω) and CuS seeds (87.84 Ω), CuS NSAs exhibited a minimum R_{CT} value (4.66 Ω), indicating the most effective mass transfer at the interface between CEs and polysulfide electrolyte. Tafel polarization profiles exhibit the limiting current density (J_{lim}) and the exchange current density (J_0). As shown in Fig. 3d, the CuS nanosheet sample with a largest slope as compared to the CuS

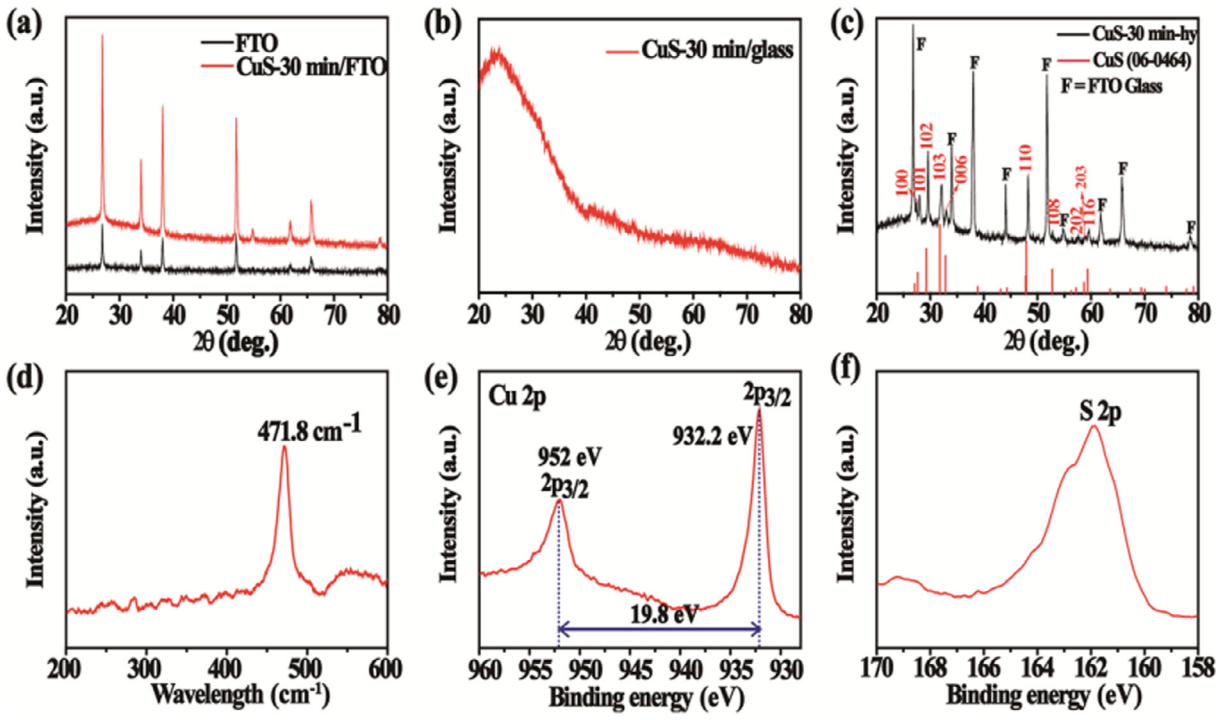

Fig. 1. XRD patterns of (a) CuS-30 min/FTO, (b) CuS-30 min/glass, (c) CuS-30 min-hy/FTO and (d) Raman spectrum of CuS-30 min-hy, and the high resolution XPS spectra of Cu 2p (e) and S2p (f).